

Neural-Network-Based Design of Approximate Gottesman-Kitaev-Preskill Code

Yexiong Zeng^{1,2}, Wei Qin^{3,1,4,*}, Ye-Hong Chen^{5,6,1,2}, Clemens Gneiting^{1,2,†} and Franco Nori^{1,2,7,‡}

¹Theoretical Quantum Physics Laboratory, Cluster for Pioneering Research, RIKEN, Wakoshi, Saitama 351-0198, Japan

²Quantum Computing Center, RIKEN, Wakoshi, Saitama 351-0198, Japan


³Center for Joint Quantum Studies and Department of Physics, School of Science, Tianjin University, Tianjin 300350, China

⁴Tianjin Key Laboratory of Low Dimensional Materials Physics and Preparing Technology, Tianjin University, Tianjin 300350, China

⁵Fujian Key Laboratory of Quantum Information and Quantum Optics, Fuzhou University, Fuzhou 350116, China

⁶Department of Physics, Fuzhou University, Fuzhou 350116, China

⁷Department of Physics, University of Michigan, Ann Arbor, Michigan 48109-1040, USA

 (Received 7 May 2024; revised 17 October 2024; accepted 24 January 2025; published 14 February 2025)

Gottesman-Kitaev-Preskill (GKP) encoding holds promise for continuous-variable fault-tolerant quantum computing. While an ideal GKP encoding is abstract and impractical due to its nonphysical nature, approximate versions provide viable alternatives. Conventional approximate GKP codewords are superpositions of multiple large-amplitude squeezed coherent states. This feature ensures correctability against single-photon loss and dephasing at short times, but also increases the difficulty of preparing the codewords. To minimize this tradeoff, we utilize a neural network to generate optimal approximate GKP states, allowing effective error correction with just a few squeezed coherent states. We find that such optimized GKP codes outperform the best conventional ones, requiring fewer squeezed coherent states, while maintaining simple and generalized stabilizer operators. Specifically, the former outperform the latter with just *one-third* of the number of squeezed coherent states at a squeezing level of 9.55 dB. This optimization drastically decreases the complexity of codewords while improving error correctability.

DOI: [10.1103/PhysRevLett.134.060601](https://doi.org/10.1103/PhysRevLett.134.060601)

Introduction—Quantum error correction (QEC), employing syndrome measurements or environmental engineering to restore encoded quantum information, plays a pivotal role for realizing large-scale fault-tolerant quantum computing [1–9]. Notably, bosonic quantum error correction promises to enable information storage in a single bosonic mode by leveraging the infinite-dimensional Hilbert space of the mode to provide redundancy for effective error resilience [10–15]. The extended lifespan and the well-defined error model of superconducting microwave cavities offer practical experimental support for this type of coding [16–20].

Among the bosonic codes, the Gottesman-Kitaev-Preskill (GKP) code is distinguished by its performance in correcting arbitrary small oscillator displacement errors. For the ideal GKP code, such errors can be corrected by an appropriate QEC method, which exclusively involves Gaussian operations [21–29]. The ideal GKP code is a powerful concept, yet its impracticality restricts its direct application to quantum computing. Feasible finite-energy approximate GKP states are required. The commonly used approximate GKP states are superpositions of highly squeezed coherent states, which gradually approach the

ideal GKP states with increasing squeezing levels. A large squeezing, often above 9.5 dB, is required for effective QEC against single-photon loss and dephasing [30,31].

However, raising the squeezing level increasingly disperses the approximate GKP states within the Fock state space, ultimately amplifying the effect of dephasing channels [32]. For conventional GKP codes, the very small probability amplitudes of large-amplitude squeezed coherent states critically impact the simultaneous error-correctability for both dephasing and single-photon loss at short times. However, these large-amplitude components are difficult to control precisely, resulting in fundamental obstacles to producing high-quality GKP codewords with superior error correction capabilities [33–38]. In particular, their optical preparation process requires breeding large-amplitude cat states, a task complicated by low success rates, limited amplitudes, and inadequate squeezing [39–43].

In this Letter, we use neural networks to model the coefficient functions of squeezed coherent states in approximate GKP states. In this approach, the optimized GKP code aims to minimize the number of squeezed coherent states while maximizing error correctability as determined by the Knill-Laflamme (KL) criterion [44,45]. Furthermore, we ensure that the produced approximate GKP states maintain the same distance to the ideal GKP states as the best conventional GKP code defined by a fixed coefficient function with optimum parameters. We find that

*Contact author: qin.wei@tju.edu.cn

†Contact author: clemens.gneiting@riken.jp

‡Contact author: fnori@riken.jp

GKP states optimized by the neural network outperform the error correction bound set by the best conventional GKP code while significantly reducing the number of large-amplitude squeezed coherent states. For example, at a squeezing level of 9.55 dB, our optimized GKP states, with just *seven* squeezed coherent states, surpass the best conventional GKP approximation, which requires 21 squeezed coherent states. The optimized approximate GKP encoding also allows for simple stabilizer operators and quantum gates. Our approach relies on the theoretical result that finite neural networks can approximate any continuous function with arbitrary precision [46–49].

Finite-energy GKP code—We focus on the square GKP codewords, defined as the common eigenstates for the operators $S_q = \exp(i2\sqrt{\pi}\hat{q})$ and $S_p = \exp(-i2\sqrt{\pi}\hat{p})$ with a shared unit eigenvalue [50]. Here, \hat{q} and \hat{p} are quadrature coordinates of a harmonic oscillator and satisfy the commutation relation $[\hat{q}, \hat{p}] = i$. These codewords are non-normalizable and impractical. Utilizing a superposition of squeezed coherent states, however, allows us to approximate them,

$$|u_L\rangle = \frac{1}{\mathcal{N}(u)} \sum_{k=-M}^M c_k^{(u)} |\alpha_k^{(u)}, r\rangle, \quad u \in \{0, 1\}, \quad (1)$$

where $|\alpha_k^{(u)}, r\rangle$ is a squeezed coherent state with squeezing magnitude r (phase $\theta = 0$) and displacement $\alpha_k^{(u)}$, $\mathcal{N}(u)$ is the normalization coefficient, and $(2M + 1)$ is the number of squeezed coherent states. Increasing the squeezing magnitude r reduces the difference between the approximate and ideal GKP states. The coefficients $c_k^{(u)}$, as nonlinear functions of $\alpha_k^{(u)} = \sqrt{(\pi/2)}(2k + u)$ and the squeezing magnitude r , are optimizable and play a crucial role in QEC. Note that $\alpha_k^{(u)}$ is kept fixed to ensure that Eq. (1) approximates the square GKP codewords (the Wigner function is a square grid). The various choices for the nonlinear functions $c_k^{(u)}$ may offer alternatives that are superior to conventional GKP codewords. For the conventional GKP code, the coefficients $c_k^{(u)}$ are defined as $c_k^{(u)} = \exp[-\pi\zeta^2(2k + u)^2/2]$ [51–53], where ζ^{-1} describes the Gaussian envelope width [22,54]. Optimizing ζ then yields the best conventional GKP code for QEC performance.

The noise channel is represented as $\mathcal{N}_i(\hat{\rho}) = \exp(\mathcal{L}t)\hat{\rho} = \sum_i \hat{A}_i(t)\hat{\rho}\hat{A}_i^\dagger(t)$, where $\hat{A}_i(t)$ and \mathcal{L} denote the Kraus operator and Lindblad superoperator, respectively. This noise channel incorporates both single-photon loss and dephasing. In practical QEC, we focus on recovering short-term errors quickly and repeatedly. For small timescales $\kappa\tau \ll 1$ and $\kappa_\phi\tau \ll 1$, we can approximate the Kraus operators as $\hat{A}_1 = \hat{I} - (\kappa\tau/2)\hat{a}^\dagger\hat{a} - (\kappa_\phi\tau/2)(\hat{a}^\dagger\hat{a})^2$, $\hat{A}_2 = \sqrt{\kappa\tau}\hat{a}$, and $\hat{A}_3 = \sqrt{\kappa_\phi\tau}\hat{a}^\dagger\hat{a}$ [32,55], where κ (κ_ϕ) is the

rate of single-photon loss (dephasing). With increasing the squeezing, the approximate GKP codewords exhibit a more spread-out distribution in Fock space, indicating that dephasing becomes the dominant source of error [32]. Thus, finding optimal GKP codes is critical for simultaneously correcting single-photon loss and dephasing errors while maintaining a small M .

The error correctability of a code can be assessed through deviations from the KL criterion [44,45,56]. Specifically, minimizing the errors $\epsilon_{ji} = \langle 1_L | \hat{A}_j^\dagger \hat{A}_i | 1_L \rangle - \langle 0_L | \hat{A}_j^\dagger \hat{A}_i | 0_L \rangle$ ensures equal error probabilities for the two logical basis states; $\zeta_{ji} = \langle 0_L | \hat{A}_j^\dagger \hat{A}_i | 1_L \rangle$ maintains the orthogonality of the error space; $\delta = \langle 0_L | 1_L \rangle$ keeps the logical basis orthogonality. If all these errors vanish (i.e., $\epsilon_{ji}, \delta, \zeta_{ij} = 0$), the KL condition is satisfied and exact QEC is, in principle, possible [57–60]. However, achieving such exact QEC is challenging for approximate GKP codes at finite squeezing levels. Realistically, errors in the approximate GKP code space caused by single-photon loss and dephasing channels can only be incompletely corrected on actual experimental platforms. Therefore, our goal is to find codewords that satisfy the KL condition to the greatest extent possible, which is equivalent to maximizing QEC performance in an error correction cycle. Consequently, we define the loss function

$$L_{\text{er}} = |\delta| + \sum_{ij} (|\epsilon_{ji}| + |\zeta_{ij}|). \quad (2)$$

We evaluate $\langle u_L | \hat{S}_q | u_L \rangle$ and $\langle u_L | \hat{S}_p | u_L \rangle$ to gauge the difference between the approximate and ideal GKP code, and find

$$\langle u_L | \hat{S}_q | u_L \rangle = \exp(-\pi e^{-2r}). \quad (3)$$

This value is solely determined by the squeezing parameter r and unaffected by M or the coefficients $c_k^{(u)}$. It implies that the approximation with a few squeezed coherent states can be as effective as utilizing many. However, $\langle u_L | \hat{S}_p | u_L \rangle$ depends on M and $c_k^{(u)}$, necessitating an additional cost function,

$$L_{\text{eg}} = \sum_{u=0,1} \max(0, \exp(-\pi e^{-2r}) - \langle u_L | \hat{S}_p | u_L \rangle), \quad (4)$$

to ensure that $|u_L\rangle$ are the approximate eigenstates of \hat{S}_p and keep the comparability with the conventional codes. Note that the ideal stabilizers only roughly stabilize the approximate codes at finite squeezing levels. Therefore, we consider more precise stabilizer operators,

$$\begin{aligned} \hat{S}_{q,\text{ap}} &= \exp[i2\sqrt{\pi}(f_{11}\hat{q} + f_{12}\hat{p})], \\ \hat{S}_{p,\text{ap}} &= \exp[-i2\sqrt{\pi}(f_{21}\hat{q} + f_{22}\hat{p})], \end{aligned} \quad (5)$$

with a complex coefficient vector $\mathbf{f} = [f_{11}, f_{12}, f_{21}, f_{22}]$. We impose the condition $f_{11}f_{22} - f_{12}f_{21} = 1$ to preserve the relation $\hat{S}_{q,\text{ap}}\hat{S}_{p,\text{ap}} = \hat{S}_{p,\text{ap}}\hat{S}_{q,\text{ap}}$. We thus define the loss function

$$L_{\text{st}} = \sum_{u=0,1} \sum_{\hat{O}} |1 - \langle u_L | \hat{O} | u_L \rangle|^2, \quad (6)$$

which ensures that the approximate GKP codewords are eigenstates of Eq. (5) with eigenvalue one, where $\hat{O} \in \{\hat{S}_{q,\text{ap}}, \hat{S}_{p,\text{ap}}, \hat{S}_{q,\text{ap}}^\dagger \hat{S}_{q,\text{ap}}, \hat{S}_{p,\text{ap}}^\dagger \hat{S}_{p,\text{ap}}\}$. The resulting total loss function, then, reads

$$L_{\text{tot}} = (1 - \eta_1 - \eta_2) \bar{L}_{\text{er}} + \eta_1 L_{\text{st}} + \eta_2 L_{\text{eg}}, \quad 0 < \eta_{1,2} < 1, \quad (7)$$

where $\bar{L}_{\text{er}} = (1/N) \sum_{\kappa\tau, \kappa_\phi\tau} L_{\text{er}}$ probes various timescales $\kappa\tau$ and $\kappa_\phi\tau$ to ensure that the codewords maintain a good error correctability over a broad time span, and N is the number of terms summed over in \bar{L}_{er} . Note that we possess an exact analytical expression for the loss function in Eq. (7), avoiding the need for numerical truncation and diminishing computational cost, especially for highly squeezed codewords [32].

Our protocol is illustrated schematically in Fig. 1. With the initial \mathbf{f} and network parameters chosen randomly, the neural network captures the complex nonlinear function $c_k^{(u)}[\beta_k^{(u)}, u, k]$, yielding a neural network-based quantum state, where $\beta_k^{(u)} = \cosh(r)\alpha_k^{(u)} + \sinh(r)\alpha_k^{(u)*}$ represents the two-photon coherent parameters for convenient computation [32,61]. Optimizing the neural network and the coefficient matrix \mathbf{f} by minimizing the loss function in Eq. (7) promises improved GKP codes. Note that we optimize the neural network instead of directly optimizing $c_k^{(u)}$ to achieve a fair comparison with the conventional GKP code, which maintains a specific relation between $c_k^{(u)}$ and $[\beta_k^{(u)}, u, k]$. Here, we use the Adam optimizer with the CosineAnnealingWarmRestarts algorithm in PyTorch to optimize the neural network and minimize the risk of getting stuck in local minima. After finding the optimum

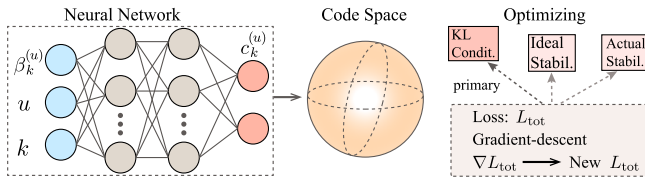


FIG. 1. Diagram of the code optimization process. The output of the neural network contains the real and imaginary components of the coefficients $c_k^{(u)}[\beta_k^{(u)}, u, k]$, and the corresponding input parameters are $[\beta_k^{(u)}, u, k]$, while keeping M constant. The gradient-based optimization of the loss function L_{tot} determines the coefficients $c_k^{(u)}[\beta_k^{(u)}, u, k]$.

codewords, we search for the optimal recovery channel $\mathcal{R}_{\text{opt}}(\cdot)$ to examine the error-correction performance of this encoding. Maximizing the channel fidelity $F = (1/4) \sum_{ij} |\text{Tr}(\hat{R}_j \hat{A}_i)|^2$ is a convex optimization problem with semidefinite constraints, where \hat{R}_j is the recovery operator [62–65]. This recover channel represents the upper boundary for QEC. We employ the QuTip library to solve the associated master equation [66–69] and the Cvxpy library for the semidefinite convex optimization in PYTHON [70,71].

Learning outcomes—We optimize the quantum states with $r = 1.1$, for example, where $r = 1.1$ corresponds to the squeezing level ≈ 9.5 dB attainable in current experiments [30,33,34]. After a meta parameters exploration, we settle for two hidden layers, each containing five neurons. The learning rate and (η_1, η_2) are 10^{-4} and $(0.02, 0.02)$, respectively. The optimized GKP code with $M = 3$ (i.e., *seven squeezed coherent states*) exhibits a significantly lower value of the loss function \bar{L}_{er} than the conventional code with $M = 10$ (i.e., *21 squeezed coherent states*), as shown in Fig. 2(a). The conventional code’s QEC ability improves as M increases, but it has an upper bound due to the constraints on the squeezing magnitude r and the fixed envelope. Surprisingly, we find that the envelope exceeds this threshold and significantly decreases the number of superposed squeezed states. The optimal coefficients are listed in Table I.

The fidelity between ideal and approximate GKP states consistently surpasses the predefined threshold of $\exp(-\pi e^{-2r})$ for $M \geq 2$ [see Fig. 2(b)]. It follows that the optimal GKP code represents an approximation to the ideal GKP code comparable to the conventional GKP code while drastically reducing the number of squeezed coherent states. The average gain $\bar{G} = \bar{L}_{\text{er}}(\text{cgkp})/\bar{L}_{\text{er}}(\text{ogkp})$, proportional to the infidelity ratio, consistently exceeds one [see Fig. 2(c)]. Hence, the optimal GKP codes are robust across a wide range of $\kappa\tau$ and $\kappa_\phi\tau$ values, beyond those involved in the training process. Moreover, the optimal GKP code at ≈ 9.5 dB consistently outperforms the best conventional GKP code across a wide squeezing range of $8 \sim 10$ dB, keeping it approximately optimal without additional neural network retraining [see Fig. 2(d)]. Notably, reoptimizing the neural network may yield even better results. Similarly, when the coefficients are constrained to the real-number domain, our conclusions still hold, albeit with diminished performance compared to the complex coefficients [32].

The optimized GKP encoding minimizes unnecessary large-amplitude squeezed coherent state components by optimizing the envelope distribution [see Figs. 2(e)–2(h)]. Note that ζ is separately optimized for fixed r to obtain the best conventional GKP code. Therefore, the code exhibits a bias between \hat{p} and \hat{q} accounting for dephasing errors, unlike the special conventional GKP code [$\zeta = \Delta = \exp(-r)$], which lacks this bias and thus performs worse under

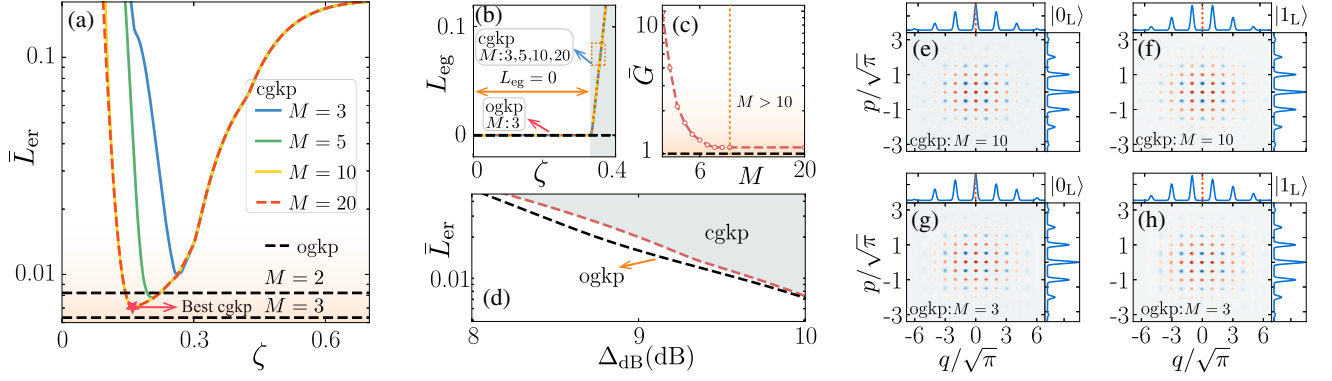


FIG. 2. The losses \bar{L}_{er} and L_{eg} for conventional GKP code versus ζ in panels (a) and (b), respectively. The black dotted lines correspond to the optimal GKP code. Note that we split here L_{tot} into its components \bar{L}_{er} and L_{eg} to highlight their physical interpretation. The timescales $\kappa\tau$ and $\kappa_\phi\tau$ lie within the range $[0, 0.005]$, with a squeezing strength of $\Delta_{\text{dB}} \approx 9.55$ dB. (c) The gain \bar{G} , defined as the ratio associated with L_{er} , derived from the optimal GKP code ($M = 3$), in comparison to the most effective conventional GKP scenario given in (a). This assessment covers a larger parameter space than the training parameters (i.e., $\kappa\tau, \kappa_\phi\tau \in [0, 0.01]$). (d) Loss function \bar{L}_{er} of the optimal GKP code obtained at $\Delta_{\text{dB}} \approx 9.55$ dB against the disturbances of squeezing in the range of 8 to 10 dB, and compared to the best conventional GKP code. Panels (e),(f) and (g),(h) present the Wigner functions for the conventional and optimal codewords ($|0_L\rangle, |1_L\rangle$) for $M = 10$ and $M = 3$, respectively.

dephasing, as shown in Fig. 2(a). The momentum marginals of the Wigner functions are invariant, consistent with the description of Eq. (3). However, for the conventional GKP code, substantial squeezed coherent state components are essential to correct single-photon loss and dephasing, even if these are small disturbances. In particular, minor coefficient perturbations can substantially deteriorate the QEC ability in the conventional GKP code, while the optimized GKP code is more robust [32]. The optimal codewords significantly mitigate the challenge of preparing the encoded states by substantially reducing the need for generating large-amplitude cat states in optical systems and the dependence on precise control in superconducting systems [33–35,39–43].

The operators in Eq. (5) can approximately stabilize the codewords, as indicated by the loss function $L_{\text{st}} \approx 1.6 \times 10^{-3}$, with each term in Eq. (6) reaching 10^{-4} . The corresponding coefficient matrix is

$$f = \begin{bmatrix} 1.000214 + 0.000054i & -0.000001 + 0.110828i \\ 0.002603 - 0.025265i & 1.002585 + 0.00023i \end{bmatrix},$$

which describes a small deviation from the ideal stabilizer operators. Additionally, the values $\langle u | \hat{\sigma}_z | u \rangle \approx (-1)^u 0.99$, $\langle u | \hat{\sigma}_x | v \rangle \approx 0.99$ ($u \neq v$), and $\|\hat{\sigma}_{x/z} | u \rangle\| \approx 1$ suggest that the Pauli operators are given by $\hat{\sigma}_z = \hat{S}_{q,\text{ap}}^{1/2}$ and $\hat{\sigma}_x = \hat{S}_{p,\text{ap}}^{1/2}$. We

can thus use the operators $\hat{d}_1 = \ln(\hat{S}_{q,\text{aq}})$ and $\hat{d}_2 = \ln(\hat{S}_{p,\text{aq}})$ coupled with an auxiliary qubit to effectively design the stabilizer protocols, where $\hat{d}_j | u_L \rangle \approx 0$. The Hamiltonian is $\hat{H} = \hat{d}_j \hat{b}_i^\dagger + \hat{d}_i^\dagger \hat{b}_j$, where \hat{b}_i describes a highly dissipative auxiliary system. Applying the Trotter decomposition to the unitary operator $\hat{U} = \mathcal{T} \exp(-i \int_0^t \hat{H}(\tau) d\tau)$, we obtain the Big-Small-Big and Small-Big-Small protocols [72]. Optimized codes with other squeezing levels or real coefficients share the same stabilizer operators in Eq. (5), with the sole difference being the coefficient matrix \mathbf{f} [32].

Quantum error correction across multiple cycles—A single QEC cycle can only protect information over a short duration; multiple cycles are required to uphold the encoded information for a long time. We evaluate the optimized GKP encoding and the best conventional GKP code for a multiple error correction process. The entire QEC procedure can be expressed as

$$\mathcal{E}^{N_c}(\hat{\rho}) = (\mathcal{R} \circ \mathcal{N})^{N_c}(\hat{\rho}), \quad (8)$$

where N_c represents the number of QEC cycles. We obtain the optimal recovery channel (which puts an upper bound on the achievable fidelity) by solving a semidefinite convex optimization problem [11,32,73,74]. Additionally, the

TABLE I. Real and imaginary parts of the optimal coefficients $c_k^{(u)}[\beta_k^{(u)}, u, k]/\mathcal{N}(u)$.

$\text{Re}[c^{(0)}]/\mathcal{N}(0)$	0.053 086	0.227 33	0.314 502	0.349 696	0.281 129	0.227 219	0.100 26
$\text{Im}[c^{(0)}]/\mathcal{N}(0)$	-0.069 034	-0.219 535	-0.280 702	-0.318 202	-0.254 336	-0.216 339	-0.112 28
$\text{Re}[c^{(1)}]/\mathcal{N}(1)$	0.124 631	0.243 408	0.300 107	0.278 471	0.230 698	0.163 76	0.009 765
$\text{Im}[c^{(1)}]/\mathcal{N}(1)$	-0.128 982	-0.226 925	-0.272 479	-0.251 869	-0.200 419	-0.137 301	-0.053 407

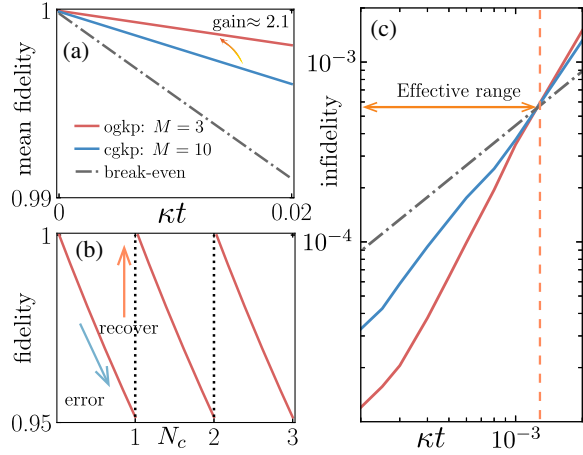


FIG. 3. (a) Mean fidelity evolution for 50 error correction with $\kappa\tau = 0.0004$ and $\kappa_\phi\tau = 0.0004/1.5$. The gain, defined as the infidelity ratio between the conventional and optimal GKP code, indicates the recovery operation efficiency achieved through convex problem solving. (b) Fidelity fluctuations during the error and recovery processes for the initial state $(|0_L\rangle + |1_L\rangle)/\sqrt{2}$ within the code space. This offers a detailed portrayal of the recovery processes for the optimal GKP code as shown in (a). (c) Comparison of the wider timescales for the QEC boundary between the optimal and conventional codewords in a single QEC cycle with $\kappa/\kappa_\phi = 1.5$.

dephasing rate is typically lower than the single-photon loss, as demonstrated in experiments with $\kappa/\kappa_\phi \approx 1.5$ [30]. Hence, we choose this ratio to determine the mean fidelity versus N_c under the optimal recovery channel. The mean fidelity is estimated using the six-point intersection of the coherent Bloch sphere face and axis [11].

As shown in Fig. 3(a), the optimized GKP encoding has a gain of ≈ 2.1 compared to the best conventional GKP code for a reasonable timescale. In Fig. 3(b), we depict how the fidelity evolves from a specific initial state throughout three error correction cycles. Specifically, the encoded state evolves freely over a short period of time, resulting in errors and a slow fidelity decrease. After a specific time interval, errors are detected, followed by a recovery procedure that restores the fidelity to a value near one. This error correction cycle is conducted iteratively to ensure long-term data storage. Figure 3(c) demonstrates that the optimal codewords achieve a higher upper bound compared to the conventional ones, enabling greater error tolerance in imperfect recovery processes across various timescales within the effective range, where the performance exceeds the breakeven point (at which logical qubits begin to outperform physical qubits).

Discussion—We used a neural network to find the optimal GKP code when the encoded system suffers single-photon loss and dephasing. Our results show that the optimized GKP encoding requires just one-third of the number of squeezed coherent states of the best conventional GKP code to achieve better QEC ability and retain

the general and simple stabilizer operators. These squeezed coherent states are arranged in close vicinity to the squeezed vacuum state, eliminating the need for numerous large-amplitude squeezed coherent states. Consequently, the optimized codewords substantially reduce the challenges of the state preparation, offering a superior alternative to conventional GKP codes. Additionally, our method can be adapted to other types of GKP codes, such as rectangular and hexagonal GKP codes, and it can serve as a reference for future corrections of single-photon loss and dephasing, as well as for developing new codes with simplified gate operations. In conclusion, our technique may significantly reduce the threshold for continuous-variable error correction.

Acknowledgments—F. N. is supported in part by Nippon Telegraph and Telephone Corporation (NTT) Research, the Japan Science and Technology Agency (JST) [via the CREST Quantum Frontiers program Grant No. JPMJCR24I2, the Quantum Leap Flagship Program (Q-LEAP), and the Moonshot R&D Grant No. JPMJMS2061], and the Office of Naval Research (ONR) Global (via Grant No. N62909-23-1-2074). C. G. is partly supported by RIKEN Incentive Research Projects. W. Q. acknowledges support of the National Natural Science Foundation of China (NSFC) (via Grants No. 0401260012 and No. 62131002). Y.-H. C. was supported by the National Natural Science Foundation of China under Grant No. 12304390.

-
- [1] J. Chiaverini, D. Leibfried, T. Schaetz, M. D. Barrett, R. B. Blakestad, J. Britton, W. M. Itano, J. D. Jost, E. Knill, C. Langer, R. Ozeri, and D. J. Wineland, Realization of quantum error correction, *Nature (London)* **432**, 602 (2004).
 - [2] P. Schindler, J. T. Barreiro, T. Monz, V. Nebendahl, D. Nigg, M. Chwalla, M. Hennrich, and R. Blatt, Experimental repetitive quantum error correction, *Science* **332**, 1059 (2011).
 - [3] D. A. Lidar and T. A. Brun, *Quantum Error Correction* (Cambridge University Press, Cambridge, England, 2013).
 - [4] B. M. Terhal, Quantum error correction for quantum memories, *Rev. Mod. Phys.* **87**, 307 (2015).
 - [5] F. Gaitan, *Quantum Error Correction and Fault Tolerant Quantum Computing* (Taylor & Francis, Andover, England, UK, 2017).
 - [6] H. Mabuchi and P. Zoller, Inversion of quantum jumps in quantum optical systems under continuous observation, *Phys. Rev. Lett.* **76**, 3108 (1996).
 - [7] J. P. Barnes and W. S. Warren, Automatic quantum error correction, *Phys. Rev. Lett.* **85**, 856 (2000).
 - [8] J. Kerckhoff, H. I. Nurdin, D. S. Pavlichin, and H. Mabuchi, Designing quantum memories with embedded control: Photonic circuits for autonomous quantum error correction, *Phys. Rev. Lett.* **105**, 040502 (2010).
 - [9] R. Lescanne, M. Villiers, T. Peronin, A. Sarlette, M. Delbecq, B. Huard, T. Kontos, M. Mirrahimi, and Z. Leghtas,

- Exponential suppression of bit-flips in a qubit encoded in an oscillator, *Nat. Phys.* **16**, 509 (2020).
- [10] I. L. Chuang, D. W. Leung, and Y. Yamamoto, Bosonic quantum codes for amplitude damping, *Phys. Rev. A* **56**, 1114 (1997).
- [11] Y. Zeng, Z.-Y. Zhou, E. Rinaldi, C. Gneiting, and F. Nori, Approximate autonomous quantum error correction with reinforcement learning, *Phys. Rev. Lett.* **131**, 050601 (2023).
- [12] T. Matsuura, H. Yamasaki, and M. Koashi, Equivalence of approximate Gottesman-Kitaev-Preskill codes, *Phys. Rev. A* **102**, 032408 (2020).
- [13] Y. Ma, Y. Xu, X. Mu, W. Cai, L. Hu, W. Wang, X. Pan, H. Wang, Y. P. Song, C.-L. Zou, and L. Sun, Error-transparent operations on a logical qubit protected by quantum error correction, *Nat. Phys.* **16**, 827 (2020).
- [14] Z. Ni, S. Li, X. Deng, Y. Cai, L. Zhang, W. Wang, Z.-B. Yang, H. Yu, F. Yan, S. Liu, C.-L. Zou, L. Sun, S.-B. Zheng, Y. Xu, and D. Yu, Beating the break-even point with a discrete-variable-encoded logical qubit, *Nature (London)* **616**, 56 (2023).
- [15] Z. Wang, T. Rajabzadeh, N. Lee, and A. H. Safavi-Naeini, Automated discovery of autonomous quantum error correction schemes, *PRX Quantum* **3**, 020302 (2022).
- [16] J. Q. You and F. Nori, Atomic physics and quantum optics using superconducting circuits, *Nature (London)* **474**, 589 (2011).
- [17] Z.-L. Xiang, S. Ashhab, J. Q. You, and F. Nori, Hybrid quantum circuits: Superconducting circuits interacting with other quantum systems, *Rev. Mod. Phys.* **85**, 623 (2013).
- [18] J. Q. You and F. Nori, Quantum information processing with superconducting qubits in a microwave field, *Phys. Rev. B* **68**, 064509 (2003).
- [19] N. Ofek, A. Petrenko, R. Heeres, P. Reinhold, Z. Leghtas, B. Vlastakis, Y. Liu, L. Frunzio, S. M. Girvin, L. Jiang, M. Mirrahimi, M. H. Devoret, and R. J. Schoelkopf, Extending the lifetime of a quantum bit with error correction in superconducting circuits, *Nature (London)* **536**, 441 (2016).
- [20] S. Krastanov, M. Heuck, J. H. Shapiro, P. Narang, D. R. Englund, and K. Jacobs, Room-temperature photonic logical qubits via second-order nonlinearities, *Nat. Commun.* **12**, 191 (2021).
- [21] D. Gottesman, A. Kitaev, and J. Preskill, Encoding a qubit in an oscillator, *Phys. Rev. A* **64**, 012310 (2001).
- [22] I. Tzitrin, J. E. Bourassa, N. C. Menicucci, and K. K. Sabapathy, Progress towards practical qubit computation using approximate Gottesman-Kitaev-Preskill codes, *Phys. Rev. A* **101**, 032315 (2020).
- [23] Y. Zheng, A. Ferraro, A. F. Kockum, and G. Ferrini, Gaussian conversion protocol for heralded generation of generalized Gottesman-Kitaev-Preskill states, *Phys. Rev. A* **108**, 012603 (2023).
- [24] M. H. Michael, M. Silveri, R. T. Brierley, V. V. Albert, J. Salmilehto, L. Jiang, and S. M. Girvin, New class of quantum error-correcting codes for a bosonic mode, *Phys. Rev. X* **6**, 031006 (2016).
- [25] T. Hillmann, F. Quijandría, A. L. Grimsmo, and G. Ferrini, Performance of teleportation-based error-correction circuits for bosonic codes with noisy measurements, *PRX Quantum* **3**, 020334 (2022).
- [26] V. V. Albert, K. Noh, K. Duivenvoorden, D. J. Young, R. T. Brierley *et al.*, Performance and structure of single-mode bosonic codes, *Phys. Rev. A* **97**, 032346 (2018).
- [27] K. Fukui, T. Matsuura, and N. C. Menicucci, Efficient concatenated bosonic code for additive Gaussian noise, *Phys. Rev. Lett.* **131**, 170603 (2023).
- [28] S. Heußen, D. F. Locher, and M. Müller, Measurement-free fault-tolerant quantum error correction in near-term devices, *PRX Quantum* **5**, 010333 (2024).
- [29] X. C. Kolesnikow, R. W. Bomantara, A. C. Doherty, and A. L. Grimsmo, Gottesman-Kitaev-Preskill state preparation using periodic driving, *Phys. Rev. Lett.* **132**, 130605 (2024).
- [30] V. V. Sivak, A. Eickbusch, B. Royer, S. Singh, I. Tsioutsios, S. Ganjam, A. Miano, B. L. Brock, A. Z. Ding, L. Frunzio, S. M. Girvin, R. J. Schoelkopf, and M. H. Devoret, Real-time quantum error correction beyond break-even, *Nature (London)* **616**, 50 (2023).
- [31] M. V. Larsen, C. Chamberland, K. Noh, J. S. Neergaard-Nielsen, and U. L. Andersen, Fault-tolerant continuous-variable measurement-based quantum computation architecture, *PRX Quantum* **2**, 030325 (2021).
- [32] See Supplemental Material at <http://link.aps.org/supplemental/10.1103/PhysRevLett.134.060601> for more details.
- [33] B. de Neeve, T.-L. Nguyen, T. Behrle, and J. P. Home, Error correction of a logical grid state qubit by dissipative pumping, *Nat. Phys.* **18**, 296 (2022).
- [34] P. Campagne-Ibarcq, A. Eickbusch, S. Touzard, E. Zalys-Geller, N. E. Frattini, V. V. Sivak, P. Reinhold, S. Puri, S. Shankar, R. J. Schoelkopf, L. Frunzio, M. Mirrahimi, and M. H. Devoret, Quantum error correction of a qubit encoded in grid states of an oscillator, *Nature (London)* **584**, 368 (2020).
- [35] A. Eickbusch, V. Sivak, A. Z. Ding, S. S. Elder, S. R. Jha, J. Venkatraman, B. Royer, S. M. Girvin, R. J. Schoelkopf, and M. H. Devoret, Fast universal control of an oscillator with weak dispersive coupling to a qubit, *Nat. Phys.* **18**, 1464 (2022).
- [36] M. Kudra, M. Kervinen, I. Strandberg, S. Ahmed, M. Scigliuzzo, A. Osman, D. P. Lozano, M. O. Tholén, R. Borgani, D. B. Haviland, G. Ferrini, J. Bylander, A. F. Kockum, F. Quijandría, P. Delsing, and S. Gasparinetti, Robust preparation of Wigner-negative states with optimized SNAP-displacement sequences, *PRX Quantum* **3**, 030301 (2022).
- [37] J. Hastrup, K. Park, R. Filip, and U. L. Andersen, Unconditional preparation of squeezed vacuum from Rabi interactions, *Phys. Rev. Lett.* **126**, 153602 (2021).
- [38] J. Hastrup, K. Park, J. B. Brask, R. Filip, and U. L. Andersen, Measurement-free preparation of grid states, *npj Quantum Inf.* **7**, 17 (2021).
- [39] J. Hastrup and U. L. Andersen, Protocol for generating optical Gottesman-Kitaev-Preskill states with cavity QED, *Phys. Rev. Lett.* **128**, 170503 (2022).
- [40] R. Dahan, G. Baranes, A. Gorlach, R. Ruimy, N. Rivera, and I. Kaminer, Creation of optical cat and GKP states using shaped free electrons, *Phys. Rev. X* **13**, 031001 (2023).
- [41] D. J. Weigand and B. M. Terhal, Generating grid states from Schrödinger-cat states without postselection, *Phys. Rev. A* **97**, 022341 (2018).

- [42] H. M. Vasconcelos, L. Sanz, and S. Glancy, All-optical generation of states for “Encoding a qubit in an oscillator”, *Opt. Lett.* **35**, 3261 (2010).
- [43] M. S. Winnel, J. J. Guanzon, D. Singh, and T. C. Ralph, Deterministic preparation of optical squeezed Cat and Gottesman-Kitaev-Preskill states, *Phys. Rev. Lett.* **132**, 230602 (2024).
- [44] E. Knill and R. Laflamme, Theory of quantum error-correcting codes, *Phys. Rev. A* **55**, 900 (1997).
- [45] E. Knill, R. Laflamme, and L. Viola, Theory of quantum error correction for general noise, *Phys. Rev. Lett.* **84**, 2525 (2000).
- [46] K. Hornik, Approximation capabilities of multilayer feed-forward networks, *Neural Netw.* **4**, 251 (1991).
- [47] G. Carleo, I. Cirac, K. Cranmer, L. Daudet, M. Schuld, N. Tishby, L. Vogt-Maranto, and L. Zdeborová, Machine learning and the physical sciences, *Rev. Mod. Phys.* **91**, 045002 (2019).
- [48] A. M. Palmieri, E. Kovlakov, F. Bianchi, D. Yudin, S. Straupe *et al.*, Experimental neural network enhanced quantum tomography, *npj Quantum Inf.* **6**, 20 (2020).
- [49] Y.-X. Zeng, T. Gebremariam, J. Shen, B. Xiong, and C. Li, Application of machine learning for predicting strong phonon blockade, *Appl. Phys. Lett.* **118**, 164003 (2021).
- [50] M. H. Shaw, A. C. Doherty, and A. L. Grimsmo, Stabilizer subsystem decompositions for single- and multimode Gottesman-Kitaev-Preskill codes, *PRX Quantum* **5**, 010331 (2024).
- [51] A. L. Grimsmo and S. Puri, Quantum error correction with the Gottesman-Kitaev-Preskill code, *PRX Quantum* **2**, 020101 (2021).
- [52] S. Glancy and E. Knill, Error analysis for encoding a qubit in an oscillator, *Phys. Rev. A* **73**, 012325 (2006).
- [53] K. Fukui, A. Tomita, and A. Okamoto, Analog quantum error correction with encoding a qubit into an oscillator, *Phys. Rev. Lett.* **119**, 180507 (2017).
- [54] H. Wang, Y. Xue, Y. Qu, X. Mu, and H. Ma, Multidimensional Bose quantum error correction based on neural network decoder, *npj Quantum Inf.* **8**, 134 (2022).
- [55] S. M. Girvin, Introduction to quantum error correction and fault tolerance, *SciPost Phys. Lect. Notes*, 70 (2023).
- [56] B. M. Terhal, J. Conrad, and C. Vuillot, Towards scalable bosonic quantum error correction, *Quantum Sci. Technol.* **5**, 043001 (2020).
- [57] D. W. Leung, M. A. Nielsen, I. L. Chuang, and Y. Yamamoto, Approximate quantum error correction can lead to better codes, *Phys. Rev. A* **56**, 2567 (1997).
- [58] C. Bény and O. Oreshkov, General conditions for approximate quantum error correction and near-optimal recovery channels, *Phys. Rev. Lett.* **104**, 120501 (2010).
- [59] M. Reimpell and R. F. Werner, Iterative optimization of quantum error correcting codes, *Phys. Rev. Lett.* **94**, 080501 (2005).
- [60] P. Faist, S. Nezami, V. V. Albert, G. Salton, F. Pastawski, P. Hayden, and J. Preskill, Continuous symmetries and approximate quantum error correction, *Phys. Rev. X* **10**, 041018 (2020).
- [61] H. P. Yuen, Two-photon coherent states of the radiation field, *Phys. Rev. A* **13**, 2226 (1976).
- [62] A. S. Fletcher, P. W. Shor, and M. Z. Win, Optimum quantum error recovery using semidefinite programming, *Phys. Rev. A* **75**, 012338 (2007).
- [63] R. L. Kosut and D. A. Lidar, Quantum error correction via convex optimization, *Quantum Inf. Process.* **8**, 443 (2009).
- [64] S. Taghavi, T. A. Brun, and D. A. Lidar, Optimized entanglement-assisted quantum error correction, *Phys. Rev. A* **82**, 042321 (2010).
- [65] D. S. Schlegel, F. Minganti, and V. Savona, Quantum error correction using squeezed Schrödinger cat states, *Phys. Rev. A* **106**, 022431 (2022).
- [66] J. R. Johansson, P. D. Nation, and F. Nori, QuTip: An open-source PYTHON framework for the dynamics of open quantum systems, *Comput. Phys. Commun.* **183**, 1760 (2012).
- [67] J. R. Johansson, P. D. Nation, and F. Nori, QuTip 2: A PYTHON framework for the dynamics of open quantum systems, *Comput. Phys. Commun.* **184**, 1234 (2013).
- [68] R. L. Kosut, A. Shabani, and D. A. Lidar, Robust quantum error correction via convex optimization, *Phys. Rev. Lett.* **100**, 020502 (2008).
- [69] S. Taghavi, T. A. Brun, and D. A. Lidar, Optimized entanglement-assisted quantum error correction, *Phys. Rev. A* **82**, 042321 (2010).
- [70] S. Diamond and S. Boyd, Cvxpy: A PYTHON-embedded modeling language for convex optimization, *J. Mach. Learn. Res.* **17**, 1 (2016), <http://jmlr.org/papers/v17/15-408.html>.
- [71] A. Agrawal, R. Verschueren, S. Diamond, and S. Boyd, A rewriting system for convex optimization problems, *J. Control Decis.* **5**, 42 (2018).
- [72] B. Royer, S. Singh, and S. M. Girvin, Stabilization of finite-energy Gottesman-Kitaev-Preskill states, *Phys. Rev. Lett.* **125**, 260509 (2020).
- [73] C. Cafaro and P. van Loock, Approximate quantum error correction for generalized amplitude-damping errors, *Phys. Rev. A* **89**, 022316 (2014).
- [74] K. Audenaert and B. De Moor, Optimizing completely positive maps using semidefinite programming, *Phys. Rev. A* **65**, 030302(R) (2002).